



Prediction of Propeller Open Water Characteristics for High Speed Boat by CFD Method

Tat-Hien Le, Nguyen Quoc Y, Nguyen Thi Ngoc Hoa, Nguyen Thi Hai Ha, Vu Ngoc Bich

Abstract: Nowadays with the development of computational resources, calculating the open water characteristics of the propeller using Computational Fluid Dynamics (CFD) has been used widely at the initial design stage because of relatively accurate result, time and cost saving, in comparison with experimental approach. This paper presents the results of computational evaluation of propeller open water characteristics for high speed boat, based on steady RANSE flow model with rotating reference frame approach. The effects of mesh density, mesh generation are analyzed in order to improve obtained numerical results. The well-known Gawn propeller series, that is often used for high speed vessel is used to verify and validate the accuracy of case studies. In this study, the authors use the commercial solver Star CCM+ by SIEMENS.

Keywords: Propeller, open water, RANSE, CFD, high speed boat.

I. INTRODUCTION

Today, the development of computational resources has helped the designers and researchers solve many complicated ship hydrodynamics problem by Computational Fluid Dynamics (CFD) method. Recently, The CFD method by solving Reynold Averaged Navier Stokes Equation (RANSE) becomes more popular within ship design offices and researchers because it can give high accuracy result with reasonable computational time. This saves cost and time compared to traditional method by testing in towing tank. Moreover, the CFD method can perform the calculation in full scale, then directly giving the hydrodynamics results such as ship resistance, propeller thrust and so on. In traditional method, we have to interpolate from the results of experiment in model scale.

In terms of methods for propeller calculation and propeller designs, there are many approaches that are available: such as lifting line, lifting surface, boundary element method (BEM) and CFD (including RANSE, LES, DNS). However, as mentioned above, to analyze the flow around the propeller, RANSE method is most popular and used widely due to RANSE flow model is closer to actual flow physics [1], [2], [3], [4].

For a high speed boat, designing and selecting a proper propeller plays a vital role to make the boat reach the required speed. With the aid of RANSE CFD tool, the designers are able to predict the propeller performance characteristic and also the details phenomenon of flow around propeller serve optimization propeller design.

There are many authors who tried to do the calculation by RANSE with the conventional propeller such as Potsdam propeller [5] and got good result. Different approaches for modelling propeller rotation by RANSE method has been performed by T.N. Tu et al [7]. In this study, three methods to simulate the propeller rotation have been performed: Sliding Grid, Rotating reference frame and Rotating domain. The result provided by the author proved that Rotating reference frame method should be used for open water simulation, in terms of computational time and level of accuracy. J.M. Baltaza et al. [6] shows the impact of important parameter for CFD setup such as iterative errors, discretization errors, domain size and boundary conditions on the simulation of propeller in open water condition. The study of T.N.Tu. [7] in different turbulence models and mesh type for open water propeller calculation shows that “SST k-omega” turbulence model with hexahedral grid give better result.

The published studies above are very valuable for the researchers who are trying to do open water calculation using RANSE CFD method. However, no one has studied the open water propeller characteristic of propeller for high speed boat. This kind of propeller normally has high rotation rate, sensitive with cavitation. Thus, special treatment needs to be taken into account for open water calculation by RANSE CFD.

Therefore, this paper presents the result of hydrodynamics calculation for the propeller of high-speed boat by RANSE CFD method, in comparison with experimental result in towing tank. The well-know Gawn propeller series [8] for high speed boat is used verify and validate the accuracy of case studies. Based on the result of the authors mentioned above, the rotating reference frame method is used to simulate propeller rotation,

Revised Manuscript Received on November 30, 2019.

* Correspondence Author

Tat-Hien Le *, Hochiminh city University of Technology, Vietnam National University, Hochiminh city, Vietnam. Email: hientl@hcmut.edu.vn.

Nguyen Quoc Y, Hochiminh city University of Technology, Vietnam National University, Hochiminh city, Vietnam.

Nguyen Thi Ngoc Hoa, Hochiminh city University of Transport, Hochiminh city, Vietnam.

Nguyen Thi Hai Ha, Vietnam Maritime University, Hai Phong, Vietnam.

Vu Ngoc Bich, Hochiminh city University of Transport, Hochiminh city, Vietnam.

© The Authors. Published by Blue Eyes Intelligence Engineering and Sciences Publication (BEIESP). This is an [open access](https://creativecommons.org/licenses/by-nc-nd/4.0/) article under the CC-BY-NC-ND license [http://creativecommons.org/licenses/by-nc-nd/4.0/](https://creativecommons.org/licenses/by-nc-nd/4.0/)

“SST k-omega” turbulence model with hexahedral grid were used in this study. The simulation is carried out by commercial solver Star-CCM+.

II. GOVERNING EQUATIONS

To investigate the propeller open water characteristic, the flow around the propeller is modeled using the incompressible viscous flow. RANS equations and averaged continuity equation are used for the quantitative description of the developed turbulent flow. Those equations are given as follows [9]:

$$\frac{\partial(\rho \bar{u}_i)}{\partial t} + \frac{\partial}{\partial t}(\rho \bar{u}_i \bar{u}_j + \overline{\rho u'_i u'_j}) = -\frac{\partial \bar{p}}{\partial x_i} + \frac{\partial \bar{\tau}_{ij}}{\partial x_j} \quad (1)$$

$$\frac{\partial(\rho \bar{u}_i)}{\partial x_i} = 0 \quad (2)$$

Where: \bar{u}_i is the averaged Cartesian components of the velocity vector; ρ is the fluid density; $\overline{\rho u'_i u'_j}$ is the Reynolds stress tensor; \bar{p} is the mean pressure and $\bar{\tau}_{ij}$ is the mean viscous stress tensor defined by:

$$\bar{\tau}_{ij} = \mu \left(\frac{\partial \bar{u}_i}{\partial x_j} + \frac{\partial \bar{u}_j}{\partial x_i} \right) \quad (3)$$

where μ is the dynamic viscosity.

In order those equations (1) and (2) form a closed system of equations, a turbulence model should be applied.

A. Turbulence model

The turbulence model used in this study is the two equation SST k-omega eddy-viscosity model. The transport equations for k and omega are [10]:

$$\frac{\partial(\rho k)}{\partial t} + \frac{\partial(\rho U_i k)}{\partial x_i} = \tilde{P}_k - \beta^* \rho \omega k + \frac{\partial}{\partial x_i} \left[(\mu + \sigma_k \mu_t) \frac{\partial k}{\partial x_i} \right] \quad (4)$$

$$\frac{\partial(\rho \omega)}{\partial t} + \frac{\partial(\rho U_i \omega)}{\partial x_i} = \alpha \rho S^2 - \beta \rho \omega^2 + \frac{\partial}{\partial x_i} \left[(\mu + \sigma_\omega \mu_t) \frac{\partial \omega}{\partial x_i} \right] + 2(1 - F_1) \rho \sigma_{\omega 2} \frac{1}{\omega} \frac{\partial k}{\partial x_i} \frac{\partial \omega}{\partial x_i},$$

Where the blending function $F_1 = \tanh(\arg^4)$ given by:

$$\arg = \min \left[\max \left(\frac{\sqrt{k}}{\beta^* \omega d}, \frac{500 \mu}{\rho d^2 \omega} \right), \frac{4 \rho \sigma_{\omega 2} k}{CD_{k\omega} d^2} \right], \quad (5)$$

with $CD_{k\omega} = \max \left(2 \rho \sigma_{\omega 2} \frac{1}{\omega} \frac{\partial k}{\partial x_i} \frac{\partial \omega}{\partial x_i}, 10^{-10} \right)$ and d is the distance to the wall.

The turbulence eddy-viscosity is defined as follows:

$$\nu_t = \frac{a_1 k}{\max(a_1 \omega, SF_2)} \quad (6)$$

Where S is the invariant measure of the strain rate and F_2 is a second blending function defined by:

$$F_2 = \tanh \left[\max \left(\frac{2\sqrt{k}}{\beta^* \omega y}, \frac{500 \nu}{y^2 \omega} \right) \right] \quad (7)$$

A production limiter is used in the SST model to prevent the build-up of turbulence in stagnation regions:

$$P_k = \mu_t \frac{\partial U_i}{\partial x_j} \left(\frac{\partial U_i}{\partial x_j} + \frac{\partial U_j}{\partial x_i} \right) \rightarrow \tilde{P}_k = \min(P_k, 10 \cdot \beta^* \rho k \omega) \quad (8)$$

All constants are computed by a blend from the corresponding constants of the k-epsilon and the k-omega model via $\alpha = \alpha_1 F + \alpha_2 (1 - F)$ etc. The constants for this model are:

$$\beta^* = 0.09, \alpha_1 = 5/9, \beta_1 = 3/40, \sigma_{k1} = 0.85, \sigma_{\omega 1} = 0.5, \alpha_2 = 0.44, \beta_2 = 0.0828, \sigma_{k2} = 1, \sigma_{\omega 2} = 0.856.$$

B. Rotating Reference Frame

Rotating reference frames provide a way of modeling rigid rotations and translations as a steady-state problem, while leaving the mesh stationary. Moving reference frames can rigidly rotate, or rotate and translate, relative to the laboratory frame [12].

The velocity of fluid particles in moving frame can be expressed by:

$$\vec{v}_r = \vec{v} - \vec{u}_r \quad (9)$$

Where: $\vec{u}_r = \vec{\omega} \times \vec{r}_r$; \vec{v}_r is the velocity of fluid particles in rotating frame; \vec{v} is absolute velocity (velocity viewed in stationary frame); $\vec{\omega}$ is angular velocity of rotating frame.

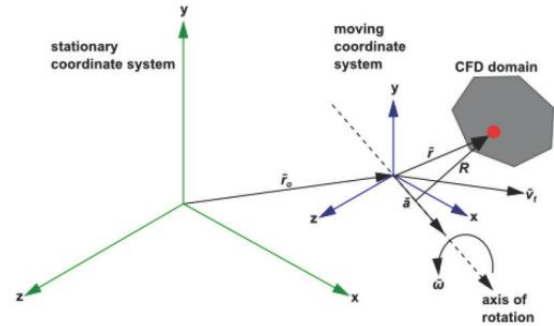


Figure.1. Description of Rotating reference frame method

The governing equation of motion written in Rotating reference frame (using \vec{v}_r instead of \vec{v}) as follows:

$$\nabla \times \rho \vec{v}_r = 0 \quad (10)$$

$$\nabla \times (\rho \vec{u}_r \vec{v}_r) + \rho (2\vec{\omega} \times \vec{v}_r + \vec{\omega} \times \vec{\omega} \times \vec{r}) = -\nabla p + \mu \nabla \times \nabla (\vec{v}_r) \quad (11)$$

In the new momentum equation, there are two additional terms $(2\vec{\omega} \times \vec{v}_r)$: Coriolis term and $\vec{\omega} \times \vec{\omega} \times \vec{r}$ centripetal acceleration term. The propeller viewed from the Rotating reference frame will be stationary.

III. NUMERICAL SIMULATION

A. Propeller model

The well-known Gawn propeller series is often used for high speed vessel. This propeller has flat face, segmental section (Figure 2).

It is quite simple to manufacture, easy to repair and have good open-water and cavitation characteristics. These are the reason that this type of propeller is using widely for small, high speed boat. This propeller series is tested extensively by Gawn in 1953 [8] for open water test and Gawn and Burrill in 1957 [13] for cavitation test.

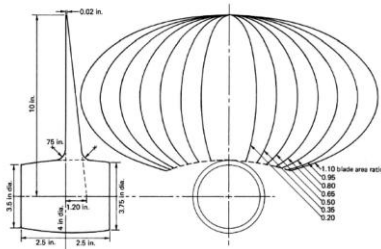


Figure 2. Blade outline of Gawn series [8]

In this paper, Gawn propeller in 3D has been modelled the by Rhinoceros software (Figure 3). This propeller has 3 blades, 20-inch diameter and right hand rotation. Detailed parameters of Gawn propeller are described in the Table 1 below.

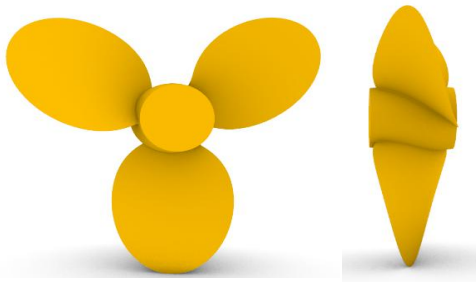


Figure 3. 3D model of Gawn propeller

Table 1. Gawn propeller parameters

Description		Unit	Value
Diameter	D	m	0.508
Pitch/Diameter at 0.7	P0.7/D	-	1
Expanded blade ratio	AE/A0	-	0.5
Hub coefficient	Dh/D	-	0.2
Blade numbers	Z	-	3
Rotation		-	Right-handed

B. Numerical Setup

The calculation of this open water simulation is performed same as experiment [8]. The range of advance coefficient J is from 0.2 to 1.0 by step 0.2. Propeller revolution is constant with 20 rps. So that advance coefficient J is changed by changing advance velocity (v_a). The environmental parameter is same as experimental set up (water density $\rho=998.67 \text{ kg/m}^3$, kinematic viscosity of water $\nu=1.070 \cdot 10^{-6} \text{ m}^2/\text{s}$ [8]).

The computation domain is a cylinder with related to propeller diameter. To avoid the influence of boundary and to capture well the propeller vortex, the outlet boundary has been extended to twelve times of propeller diameter (12D), the outlet boundary is two times of propeller diameter (2D) from the propeller plane. The diameter of domain is ten times of propeller diameter (10D). It should be noted that the selection of location of the boundaries was done based on recommendations given by ITTC [14].

Retrieval Number: A4790119119/2019©BEIESP

DOI: 10.35940/ijitee.A4790.119119

Journal Website: www.ijitee.org

The boundary conditions are: Velocity inlet at Inlet; pressure outlet at outlet and the side of cylinder is set as symmetry plane. The flow velocity is imposed at inlet with advance velocity corresponding to advance coefficient (J). For the propeller, the non-slip boundary condition is applied. So, the propeller blades, hub and shaft are set as “wall” boundary.

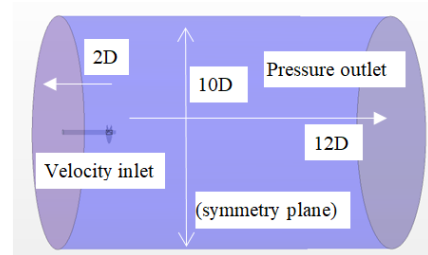


Figure 4. Computation domain and boundary condition

The mesh types are important factors that effect on numerical results. According to [7] using hexahedral grid give better results than other grid for all range of advance coefficient of propeller. So, hexahedral grid was used in this study. The mesh local refinement is applied around propeller only to avoid having large number of cells. The area behind propeller also refines to capture propeller vortex. The other important thing in mesh setup is the leading edge and trailing edge refinement. The authors have made a volume refinement around leading and trailing edges to capture the large curvature at that position. To solve the boundary layer around propeller, the prism layers are generated for resolving the boundary layer. Figure 5 and Figure 6 shows the typical mesh generation.

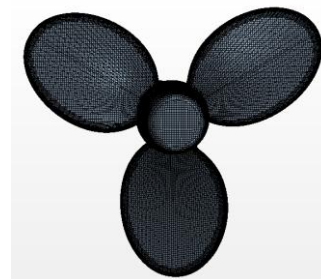
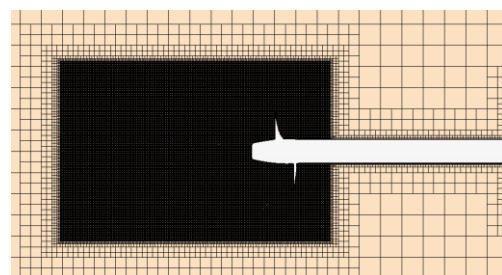


Figure 5. Mesh generation on propeller



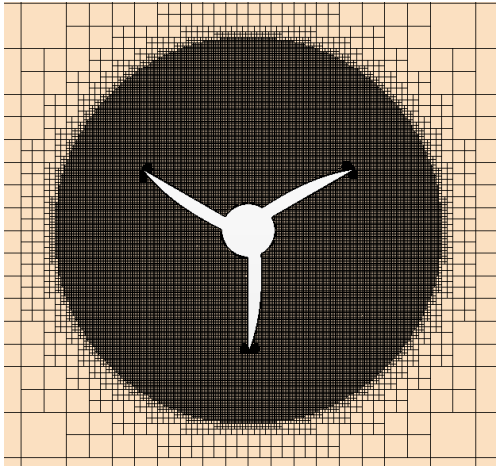


Figure 6. Mesh refinement around propeller

For propeller open water analysis, the propeller inflow is uniform, so the steady RANSE is applied to calculate flow field around propeller. Rotating reference frame approach are used in this study from the point of view computational time and level of accuracy [12]. For high speed boat, the propeller often works in high revolution rate, so the flow is fully turbulence. Thus, the turbulence model $k-\omega$ SST is used. Wall function is applied to solve boundary layer. At the area that Y^+ is low, the solver automatically changes to solve near wall boundary layer. This approach is called “All wall treatment”.

IV. CALCULATION RESULT AND DISCUSSIONS

A. Mesh convergence study

Mesh convergence study is very important in the accuracy of CFD calculation, to make sure that the mesh size is sufficient to decrease the discretization error to an acceptable level [15]. Thus, in presented case study, the mesh convergence study is performed at advance coefficient $J = 0.6$ using three grids by grid refinement ratio $r_G = \sqrt{2}$ (the value recommended by ITTC [16]). Three meshes are generated: coarse, medium and fine with the cell numbers of 2.80, 3.60 and 5.2 million cells.

The solution changes between two simulations such as fine-medium ε_{12} and medium coarse ε_{23} are defined as follow:

$$\varepsilon_{12} = (S_1 - S_2) / S_1; \varepsilon_{23} = (S_2 - S_3) / S_2 \quad (12)$$

Where: S_1, S_2, S_3 – the result of open water simulation with fine, medium and coarse mesh

Table 2 shows the result of mesh convergence study. The changes of solution from coarse mesh to fine mesh are quite significant, especially for K_T , from 5.7% to 1.8%. K_Q and η_0 also show the same behavior. It means that increasing the mesh size, the solution converged to a value. Therefore, in this case, fine mesh should be used for further calculation. Furthermore, using fine mesh helps us to visualize more detailed the flow behind the propeller, especially propeller vortex (Figure 7).

Table 2. Results of mesh convergence study at advance coefficients $J=0.60$

Characteristics	Mesh density			ε_{23} [%]	ε_{12} [%]
	Coarse grids	medium grids	fine grids		
K_T	0.211	0.223	0.227	5.7%	1.8%
$10K_Q$	0.345	0.352	0.354	2.0%	0.6%
η_0	0.605	0.611	0.612	1.0%	0.2%

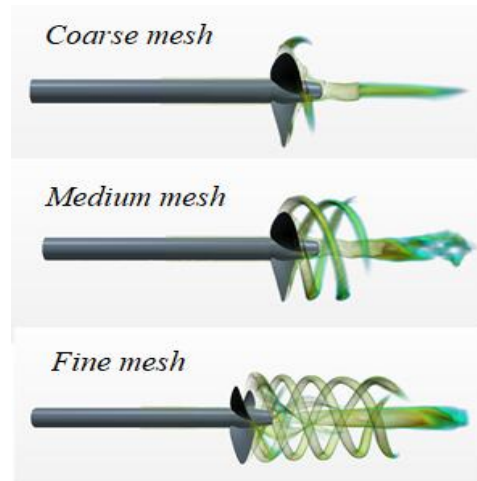


Figure 7. Vortex distribution at $J = 0.6$ for different mesh density

B. Calculation Results

Table 3 and Figure 8 present the comparison between calculated and experimental result of open water characteristics of propeller at range of advance velocity J from 0.2 to 1.0. The differences between the EFD (Experimental Fluid Dynamic) data, D , and CFD (Computational Fluid Dynamic) simulation, S in this paper is defined by:

$$E\%D = \frac{(D - S)}{D} 100\% \quad (13)$$

From the computational results (Table 3) and experimental data from [8]. Compared to the experimental data, the simulation results show good agreement with experimental values.

The RANSE CFD method not only gives us the numerical value of our interested quantity, it can give us more details about the flow around propeller such as pressure and vortex distribution. This is very useful for designers to take into account the noise, vibration and optimization in propeller design. The post-processing results are shown at Figure 7, Figure 9 and Figure 10.

Table 3. Result of open water calculation compared to experimental values

J	K_T			$10K_Q$			η_0		
	EFD	CFD	E%D [%]	EFD	CFD	E%D [%]	EFD	CFD	E%D [%]
0.2	0.380	0.398	4.7%	0.537	0.555	3.35	0.225	0.228	1.4%
0.4	0.309	0.298	-3.6%	0.450	0.430	-4.5%	0.437	0.441	0.9%
0.6	0.229	0.227	-0.8%	0.353	0.354	0.2%	0.618	0.612	-1.0%
0.8	0.142	0.136	-4.5%	0.248	0.242	-2.4%	0.729	0.715	-2.0%
1.0	0.053	0.051	-4.0%	0.136	0.130	-4.7%	0.619	0.623	0.7%

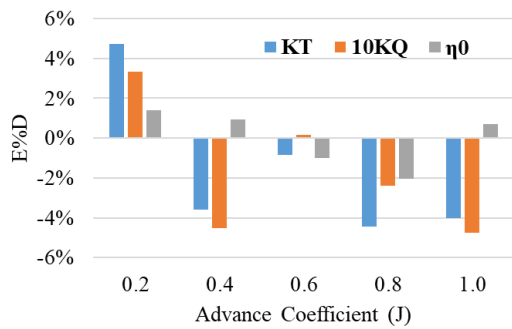
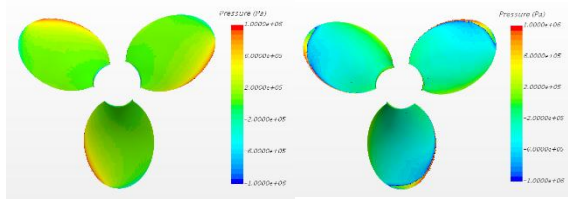
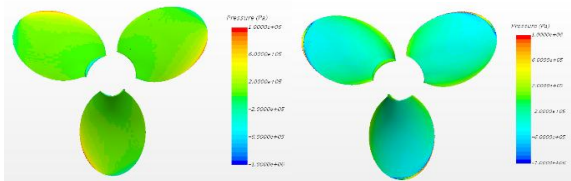


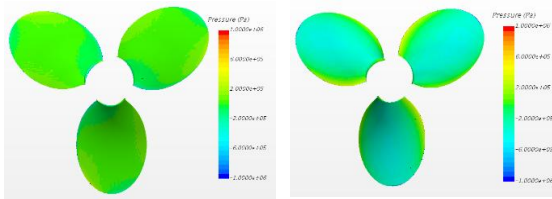
Figure 8. Comparison between CFD and EFD for open water calculation



a) Pressure distribution at $J = 0.4$ (left side: Pitch face, Right side: Back face)

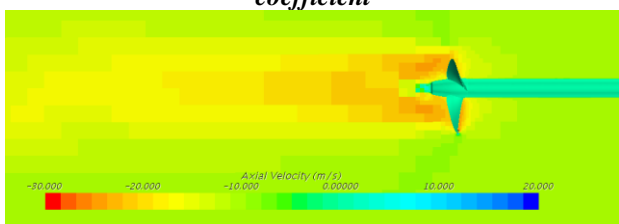


b) Pressure distribution at $J = 0.6$ (left side: Pitch face, Right side: Back face)

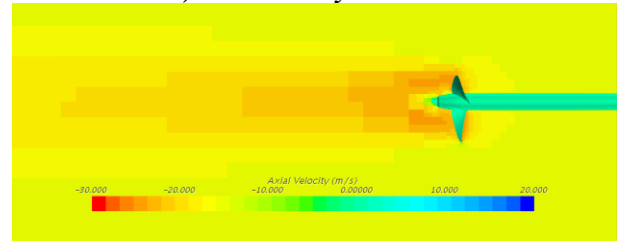


c) Pressure distribution at $J = 0.8$ (left side: Pitch face, Right side: Back face)

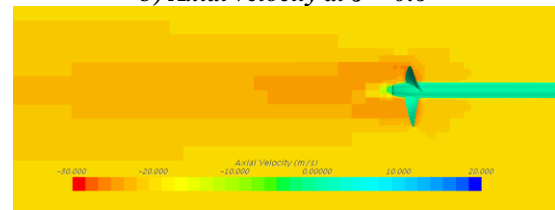
Figure 9. Pressure distribution at different advance coefficient



a) Axial velocity at $J = 0.4$



b) Axial velocity at $J = 0.6$



c) Axial velocity at $J = 0.8$

Figure 10. Axial velocity at different advance coefficient

Figure 10 shows the distribution of axial velocity of flow around propeller at $J = 0.4, 0.6$ and 0.8 . The axial velocity increases with advance coefficient J , and the flow is more turbulent. This is due to the linear relationship between advance coefficient (J) and advance velocity (v_a) when the rotation rate (n) and the propeller diameter (D) are constant.

C. Discussions

As can see in the Figure 8 and Table 3, the CFD result is well agreement with experimental result, especially for open water efficiency. The discrepancy is just about 2% for open water efficiency. This good result is obtained by correct selection of turbulence model and studying mesh convergence.

Figure 7 shows the vortex shedding behind the propeller. This image proves the capability of RANSE CFD in visualization of flow. This type of visualization was very costly in cavitation tunnel with the aid of high-speed camera.

V. CONCLUSION

In this study, the propeller open water characteristics for high speed boat have been predicted by RANSE CFD method. The results are well agreement with experimental result. This shows the important role of mesh convergence study and mesh refinement for important area of propeller blades. This study shows the capability of flow visualization by RANSE CFD method. However, to get detailed picture about the flow behind the propeller, the mesh refinement needs to be carried out at downstream of flow.

This will increase of mesh size and also raise the computational time. In case that only open water characteristics are interested, this refinement may not be necessary.

Another interested phenomenon for high speed propeller is cavitation problem. Further study should be carried out to perform cavitation prediction, which is required small mesh size and higher number of cells.

ACKNOWLEDGMENT

This research is supported by Vietnam National University Ho Chi Minh city (VNU-HCM) under grant number C2018-20-06.

REFERENCES

1. Molland, A.F., S.R. Turnock, and D.A. Hudson, *Ship resistance and propulsion*. 2017: Cambridge university press.
2. Bertram, V., *Practical ship hydrodynamics*. 2011: Elsevier.
3. Perali, P., T. Lloyd, and G. Vaz. *Comparison of uRANS and BEM-BEM for propeller pressure pulse prediction: E779A propeller in a cavitation tunnel*. in *Proceedings of the 19th Numerical Towing Tank Symposium*. 2016.
4. Brizzolara, S., D. Villa, and S. Gaggero. *A systematic comparison between RANS and panel methods for propeller analysis*. in *Proc. Of 8th International Conference on Hydrodynamics, Nantes, France*. 2008.
5. Barkmann, U., H.-J. Heinke, and L. Lübke. *Potsdam Propeller Test Case (PPTC)*. in *Proceeding of the Second International Symposium on Marine Propulsors-smp'11*. 2011.
6. Baltazar, J.M., D.R. Rijpkema, and J. Falcao De Campos. *Numerical studies for verification and validation of open-water propeller RANS computations*. in *Proceedings of the 6th International Conference on Computational Methods in Marine Engineering (Rome, Italy)*. 2015.
7. Tu, T.N., *Numerical simulation of propeller open water characteristics using RANSE method*. Alexandria Engineering Journal, 2019.
8. Gawn, R., *Effect of pitch and blade width on propeller performance*. Trans. INA, 1953. **95**: p. 157.
9. Ferziger, J.H. and M. Perić, *Computational methods for fluid dynamics*. Vol. 3. 2002: Springer.
10. Menter, F.R., M. Kuntz, and R. Langtry, *Ten years of industrial experience with the SST turbulence model*. Turbulence, heat and mass transfer, 2003. **4**(1): p. 625-632.
11. *CD-adapco, 2017. STAR-CCM+ User Guide*.
12. Tran Ngoc Tu, N.M.C., *Comparison Of Different Approaches For Calculation Of Propeller Open Water Characteristic Using RANSE Method*. Naval Engineers Journal, 2018. **Volume 130, Number 1, 1 March 2018, pp. 105-111(7)**.
13. Gawn, R. and L. Burrill, *Effect of cavitation on the performance of a series of 16" propellers.*. Transactions of the Royal Institution of Naval Architects, 1957. **99**.
14. <https://www.itc.info/media/8169/75-03-03-01.pdf>.
15. Wilcox, D.C., *Turbulence modeling for CFD*. Vol. 2. 1998: DCW industries La Canada, CA.
16. *ITTC-Quality Manual 7.5-03-01-01, 2008*

AUTHORS PROFILE



Tat-Hien Le received his Bachelor degree (2004) in Naval Architecture & Marine Engineering from Ho Chi Minh City University of Technology-Vietnam National University Ho Chi Minh City (VNU-HCM), Vietnam; M.Sc. degree (2004) and PhD degree (2009) from Pukyong National University, South Korea.

He is a Lecturer, Department of Naval Architecture & Marine Engineering, Ho Chi Minh City University of Technology-VNU-HCM. His current interests include modeling, simulation, and optimization in ship design



Nguyen Quoc Y received his Bachelor degree (2003) from Ho Chi Minh City University of Technology-Vietnam National University Ho Chi Minh City, Vietnam; M.Sc. degree (2005) and PhD degree (2008) from Ritsumeikan University, Japan.

He is a Lecturer, Faculty of Civil Engineering, Ho Chi Minh City University of Technology-VNU-HCM. His current interests include computational fluid dynamic.



Nguyen Thi Ngoc Hoa received her Bachelor degree (2002) and M.Sc. degree (2013) from Hochiminh city University of Transport.

She is a Lecturer, Department of Ship Design, Hochiminh city University of Transport. Her current interests include ship design, stability and optimization.



Nguyen Thi Hai Ha received her Bachelor degree (2006) from Vietnam Maritime University; M.Sc. degree (2010) from the cooperative program between Vietnam Maritime University and University in Liège, Belgium. She is a Lecturer, Shipbuilding Faculty, Vietnam Maritime University. Her current interests include ship design and Computational Fluid Dynamic.

Her current interests include ship design and Computational Fluid Dynamic.



Vu Ngoc Bich was born in 1961. He received PhD degree (2007) from Russia.

He is a Lecturer, Department of Ship Building, Hochiminh city University of Transport. His current interests include in ship design and optimization.